Title

50 Gb/s hybrid silicon traveling-wave electroabsorption modulator

Journal

Optics Express, 19(7)

Authors

Tang, Yongbo
Chen, Hui-Wen
Jain, Siddharth
et al.

Publication Date

2011-03-28

Peer reviewed

50 Gb/s hybrid silicon traveling-wave electroabsorption modulator

Yongbo Tang,[1,2,3*] Hui-Wen Chen,[1] Siddharth Jain,[1] Jonathan D. Peters, [1] Urban Westergren, [2,3] and John E. Bowers[1]

[1]*Department of Electrical and Computer Engineering, University of California Santa Barbara, Santa Barbara, CA 93106, USA*
[2]*KTH-ZJU Joint Research Center of Photonics, Zhejiang University, Hangzhou 310058, China*
[3]*Department of Microelecronics and Applied Physics, Royal Institute of Technology (Sweden), Kista 16440, Sweden*
**ytang@ece.ucsb.edu*

Abstract: We have demonstrated a traveling-wave electroabsorption modulator based on the hybrid silicon platform. For a device with a 100 μm active segment, the small-signal electro/optical response renders a 3 dB bandwidth of around 42 GHz and its modulation efficiency reaches 23 GHz/V. A dynamic extinction ratio of 9.8 dB with a driving voltage swing of only 2 V was demonstrated at a transmission rate of 50 Gb/s. This represents a significant improvement for modulators compatible with integration of silicon-based photonic integrated circuits.

OCIS codes: (250.4410) Modulators; (250.5300) Photonic integrated circuits; (250.7360) Waveguide modulators.

References and links

1. D. Liang, G. Roelkens, R. Baets, and J. Bowers, "Hybrid integrated platforms for silicon photonics," Materials **3**(3), 1782–1802 (2010).
2. J. Michel, J. Liu, and L. Kimerling, "High-performance Ge-on-Si photodetectors," Nat. Photonics **4**(8), 527–534 (2010).
3. http://www.intel.com/pressroom/archive/releases/20100727comp_sm.htm
4. A. Liu, R. Jones, L. Liao, D. Samara-Rubio, D. Rubin, O. Cohen, R. Nicolaescu, and M. Paniccia, "A high-speed silicon optical modulator based on a metal-oxide-semiconductor capacitor," Nature **427**(6975), 615–618 (2004).
5. A. Liu, L. Liao, D. Rubin, H. Nguyen, B. Ciftcioglu, Y. Chetrit, N. Izhaky, and M. Paniccia, "High-speed optical modulation based on carrier depletion in a silicon waveguide," Opt. Express **15**(2), 660–668 (2007).
6. Q. Xu, B. Schmidt, S. Pradhan, and M. Lipson, "Micrometre-scale silicon electro-optic modulator," Nature **435**(7040), 325–327 (2005).
7. J. Basak, L. Liao, A. Liu, D. Rubin, Y. Chetrit, H. Nguyen, D. Samara-Rubio, R. Cohen, N. Izhaky, and M. Paniccia, "Developments in gigascale silicon optical modulators using free carrier dispersion mechanisms," Adv. Opt. Technol. **2008**, 1 (2008).
8. J. Liu, M. Beals, A. Pomerene, S. Bernardis, R. Sun, J. Cheng, L. Kimerling, and J. Michel, "Waveguide-integrated, ultralow-energy GeSi electroabsorption modulators," Nat. Photonics **2**(7), 433–437 (2008).
9. Y. H. Kuo, Y. K. Lee, Y. Ge, S. Ren, J. E. Roth, T. I. Kamins, D. A. Miller, and J. S. Harris, "Strong quantum-confined Stark effect in germanium quantum-well structures on silicon," Nature **437**(7063), 1334–1336 (2005).
10. D. Liang and J. Bowers, "Recent progress in lasers on silicon," Nat. Photonics **4**(8), 511–517 (2010).
11. R. Walker, "High-speed III-V semiconductor intensity modulators," IEEE J. Quantum Electron. **27**(3), 654–667 (1991).
12. R. Lewén, S. Irmscher, U. Westergren, L. Thylén, and U. Eriksson, "Segmented transmission-line electroabsorption modulators," J. Lightwave Technol. **22**(1), 172–179 (2004).
13. C. Doerr, L. Zhang, P. Winzer, J. Sinsky, A. Adamiecki, N. Sauer, and G. Raybon, "Compact High-Speed InP DQPSK Modulator," IEEE Photon. Technol. Lett. **19**(15), 1184–1186 (2007).
14. Y. Chiu, T. Wu, W. Cheng, F. Lin, and J. Bowers, "Enhanced performance in traveling-wave electroabsorption modulators based on undercut-etching the active-region," IEEE Photon. Technol. Lett. **17**(10), 2065–2067 (2005).
15. Y. H. Kuo, H. W. Chen, and J. E. Bowers, "High speed hybrid silicon evanescent electroabsorption modulator," Opt. Express **16**(13), 9936–9941 (2008).
16. F. Devaux, S. Chelles, A. Ougazzaden, A. Mircea, and J. Harmand, "Electroabsorption modulators for high-bit-rate optical communications: a comparison of strained InGaAs/InAIAs and InGaAsP/InGaAsP MQW," Semicond. Sci. Technol. **10**(7), 887–901 (1995).

#141070 - $15.00 USD Received 13 Jan 2011; revised 25 Feb 2011; accepted 4 Mar 2011; published 14 Mar 2011

17. S. Jain, M. Sysak, G. Kurczveil, and J. Bowers, "Integrated Hybrid Silicon DFB Laser-EAM array using Quantum Well Intermixing, IEEE J. Sel. Top. Quantum Electron. Submitted.
18. H. W. Chen, J. D. Peters, and J. E. Bowers, "Forty Gb/s hybrid silicon Mach-Zehnder modulator with low chirp," Opt. Express **19**(2), 1455–1460 (2011).
19. H. Boudinov, H. H. Tan, and C. Jagadish, "Electrical isolation of n-type and p-type InP layers by proton bombardment," J. Appl. Phys. **89**(10), 5343–5347 (2001).
20. F. Devaux, Y. Sorel, and J. F. Kerdiles, "Simple measurement of fiber dispersion and of chirp parameter of intensity modulated light emitter," J. Lightwave Technol. **11**(13), 1937–1940 (1993).

1. Introduction

The emerging Internet applications such as cloud computing and video-based services are calling for faster and cheaper communication within and between data centers. The challenge of current microelectronic architecture in transmission bandwidth and power consumption can be potentially solved by using high-speed optical interconnects. Silicon photonics is of interest because it uses the same substrate as and process techniques compatible with modern CMOS fabrication. This vision becomes more viable as active functionalities are improved with emerging silicon-compatible techniques based on the hybrid silicon platform [1] and the Ge-on-Si platform [2].

Recently, Intel has demonstrated a 50 Gb/s photonic transmitter consisting of four hybrid silicon lasers, four silicon modulators and an echelle grating multiplexer [3]. The modulators in this integrated four-channel wavelength-division multiplexing (WDM) transmitter operated at a speed of 12.5 Gb/s. The bandwidth of the silicon modulator is limited due to the lack of efficient electro-optic effect and electroabsorption effect in pure silicon. Most of the reported silicon modulators rely on the free carrier plasma dispersion effect [4–7]. In those cases, a weak change of the refractive index obtained by carrier accumulation, injection or depletion is utilized in a Mach-Zehnder interferometer [4,5] or a microring resonator [6] to achieve intensity modulation. 40 Gbit/s transmission has been demonstrated on a carrier-depletion-based silicon modulator, although that device has a large footprint and requires high driving voltage for a sufficient extinction ratio [7].

In order to overcome the drawbacks inherent to the silicon modulators, some other materials capable of more efficient modulation have been introduced to the silicon platform. The discovery of strong electroabsorption effect in the strained Ge/Si [8] or Ge/GeSi multiple quantum-wells [9] laid the foundation for the Ge/Si electroabsorption modulators (EAMs) but the high-speed performance of the demonstrated devices are still not competitive. Another option is to transfer the III-V epitaxial layers onto a silicon-on-insulator (SOI) wafer by using wafer bonding techniques [1]. The benefits of the hybrid silicon platform are not only efficient lasing [10] but also the possibility to transfer the state-of-the-art modulator techniques [11–14] to the silicon platform. We have earlier reported a hybrid silicon EAM with a modulation bandwidth of 16 GHz [15], whose speed is mainly limited by the lumped electrode design. In this paper, we demonstrate a new hybrid silicon EAM utilizing a traveling-wave (TW) electrode for a faster operation. The fabricated TW-EAM device reaches a high figure of merit of 23 GHz/V (defined as the ratio of the 3 dB bandwidth to the driving voltage for a 10 dB extinction ratio [16]) and it exhibits a clear opening of the eye diagram at a data rate as high as 50 Gb/s. This performance is very competitive, even when compared with its InP-based counterparts. Quantum well intermixing has been used to integrate arrays of distributed feedback lasers with hybrid silicon modulators [17], and it can be applied here to develope a compact 50 Gb/s hybrid silicon electroabsorption modulated laser (EML).

2. Device description

An EAM is usually implemented by using a pin diode structure with the active multiple quantum wells (MQW) located inside the intrinsic layer. The bias applied to the pin diode adjusts the electrical field in the MQW region and results in the change of optical absorption due to the quantum confined Stark effect (QCSE). Typically, a thin intrinsic layer is preferred to achieve a good extinction ratio, but it will lead to a large device capacitance that limits the

#141070 - $15.00 USD Received 13 Jan 2011; revised 25 Feb 2011; accepted 4 Mar 2011; published 14 Mar 2011

device's high speed performance, especially for the lumped EAM design. A traveling-wave electrode design overcomes the RC limit due to the distributed circuit configuration.

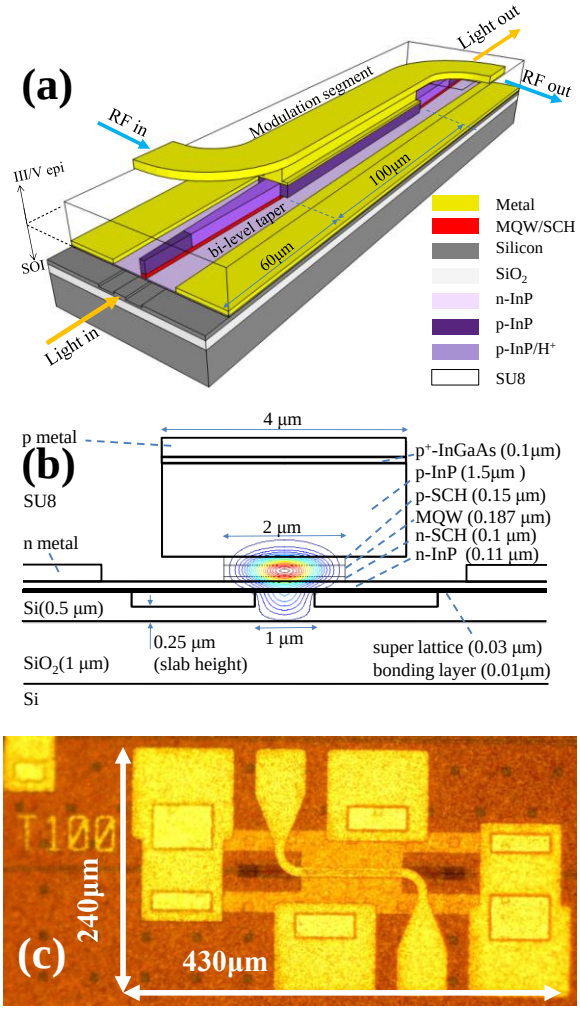

Fig. 1. (a) Schematic structure of a hybrid silicon TW-EAM. (b) Cross section of the modulation segment with a superimposed fundamental optical mode. (c) Top-view photograph of a fabricated TW-EAM.

Figure 1(a) shows the structure of the hybrid silicon traveling-wave electroabsorption modulator, with III-V epitaxial layers bonded on an SOI wafer. The SOI wafer has a 500 nm thick silicon layer and a 1 μm thick oxide layer. The III-V epitaxial layers were grown on an InP substrate. Its intrinsic layer contains an offset InGaAlAs/InGaAlAs MQW stack sandwiched by two separate confinement heterostructures (SCH). The MQW is composed of 10 compressive wells and 11 tensile barriers with its photoluminescent (PL) peak at 1478 nm. Detailed of the material parameters can be found in [15]. This configuration of the MQW is optimized for transverse electric (TE) polarization [16], appropriate for integration with a silicon-based laser.

The fabrication of this hybrid silicon TW-EAM is similar to that in [18]. The silicon ridge waveguide has a slab height of 250 nm while the ridge width varies from 1.5 μm in the passive section to 1.0 μm under the III-V mesa. Figure 1(b) depicts the cross section of the hybrid modulation segment. The p-InP mesa has a width of 4 μm, defined by using the top p-

#141070 - $15.00 USD Received 13 Jan 2011; revised 25 Feb 2011; accepted 4 Mar 2011; published 14 Mar 2011

metal (Pd/Ti/Pd/Au) as a hard mask, while the width of the intrinsic layer is reduced to 2 μm by selective under-etching in order to increase the characteristic impedance and reduce the microwave loss [14]. A 0.5 μm thick Ni/Ge/Au/Ni/Au alloy was deposited over the thin n-InP contact and formed the ground pad after lift-off process. A 5 μm thick SU8 polymer was used for passivation to decrease parasitic capacitance and gold vias were plated to connect the probe and contact metal. The top probe strip, also made by plating, has a width of 10 μm and a height of 3 μm. Ground-signal-ground (GSG) contact pads with 100 μm pitch were used for the input and output RF ports. The traveling-wave electrode configuration can be seen in the top-view photograph in Fig. 1(c). The device is very compact with a footprint of 240 μm × 430 μm including the electrode pads.

Figure 1(b) also shows the simulated fundamental optical mode for the hybrid silicon waveguide. Most of the optical power is confined in the MQW region for a higher confinement factor. The mode conversion from the silicon ridge waveguide to the hybrid silicon waveguide is achieved by a 60 μm long bi-level taper, with the III-V mesa width laterally tapered from 0.6 μm to 2.0 μm and the silicon ridge width from 1.5 μm to 1.0 μm, and vice versa. Proton (H^+) implantation was applied to part of the tapers (see Fig. 1(a)) to decrease the doping [19] so that the tapers can be electrically isolated from the modulation segment.

3. Device characteristics

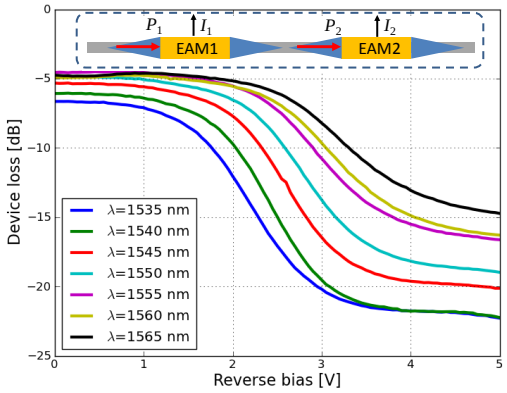

Fig. 2. Device loss of a hybrid silicon TW-EAM under different biases. The inset shows the schematic of the testing structure for the loss measurement.

We characterize the device loss by using a set of cascaded EAMs as shown in the inset of Fig. 2. The input optical powers reaching the two modulators are labeled as P_1 and P_2, respectivley. They are proportional to the photocurrents extracted from the modulators. Supposing that the two EAMs are identical, the device loss of one EAM can be approximately obtained by:

$$Loss(dB) = 10\log_{10}(\frac{P_2}{P_1}) = 10\log_{10}(\frac{I_2}{I_1}), \quad (1)$$

where I_1 and I_2 are the photocurrents simultaneously extracted from the two modulators under the same bias. Note that the loss from two tapers and the connecting silicon waveguide is included. Based on this method, we measured the bias-dependent device loss for a hybrid silicon TW-EAM with an active length of 100 μm. During the measurement, the polarization of the input light is optimized by using a polarization controller to have a maximal photocurrent. It corresponds to the TE polarization, which is verified by checking the output optical spot through a crystal polarization beam splitter. Figure 2 shows a group of loss curves

#141070 - $15.00 USD Received 13 Jan 2011; revised 25 Feb 2011; accepted 4 Mar 2011; published 14 Mar 2011

obtained at different input wavelengths from 1535 nm to 1565 nm. We can see that the unbiased loss keeps reducing until the wavelength increased to 1550 nm, implying that the static material absorption is no longer an issue at a longer wavelength. The on-chip loss at 1550 nm is around 5 dB, larger than that of the previously reported lumped device (3dB in [15]). We believe that it mainly comes from the mode transition loss in the taper and the free carrier absorption due to the proton bombardment. Increasing the taper length and reducing the implantation area could help reduce the device loss. We can also see the steady-state extinction ratio from Fig. 2. For the wavelength of 1550 nm, more than 11 dB extinction ratio is achieved with a voltage change from –2 V to –4 V. Shorter wavelength gives a better extinction ratio and a reduced optimal bias but an increased on-chip loss.

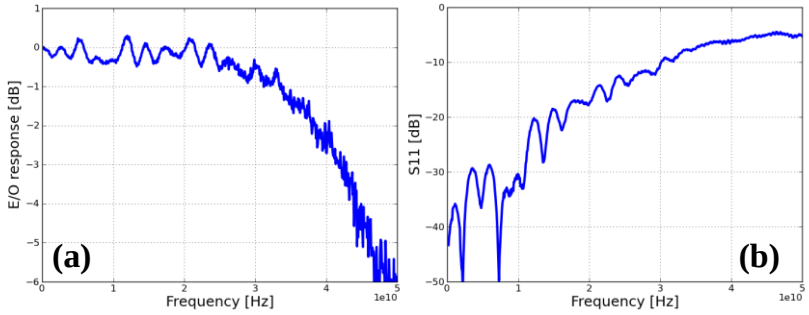

Fig. 3. (a) Small signal E/O response and (b) the microwave reflection to the RF source (S_{11}) for a hybrid silicon TW-EAM with a 100 μm active segment.

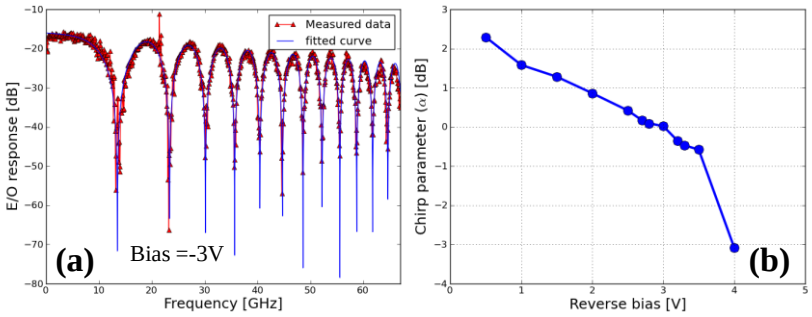

Fig. 4. (a) E/O response with –3V bias for chirp measurement; (b) Chirp parameters at different biases. A 27.92 km single-mode fiber was used.

The small-signal modulation of a hybrid silicon TW-EAM was measured by using a lightwave component analyzer (Agilent N4373A), where a GSG probe capped with a standard 50 Ω off-chip terminator was attached to the output port of the device. Figure 3 shows the electro/optical (E/O) modulation response and the microwave reflection (S_{11}) to the RF source for one device under a bias of –3 V. The measurement indicates an E/O 3dBe bandwidth as high as 42 GHz and less than –10 dB microwave reflection up to 30 GHz. Five out of eight 100 μm TW-EAM samples under E/O testing have a bandwidth over 40 GHz. We also measured the chirp parameters of the modulator by inserting a 27.92 km single-mode fiber between the modulator and the detector [20]. The dispersion of the fiber and the chirp induced by the modulator will introduce resonance dips to the E/O response like the one shown in Fig. 4(a). Based on those dips, the chirp parameters were extracted and summarized in Fig. 4(b). We can see that chirp-free operation can be achieved under a bias around –3 V.

In order to evaluate the large signal performance, a non-return-to-zero (NRZ) pseudorandom bit sequence (PRBS) pattern with a word length of 2^{31}-1, generated by an SHF

#141070 - $15.00 USD Received 13 Jan 2011; revised 25 Feb 2011; accepted 4 Mar 2011; published 14 Mar 2011

BERT and amplified to a level of 2 V swing, was applied to the TW-EAM sample under a bias of −3 V. The modulated optical signal was collected by a lensed fiber and amplified by an erbium doped fiber amplifier (EDFA) followed by a 200 GHz bandpass optical filter to suppress the amplified spontaneous emission (ASE) noise. The optical signal was detected by a 50 GHz photodetector mounted on an Agilent digital communication analyzer (DCA). As shown in Fig. 5, a clear eye opening was observed at 50 Gb/s with a dynamic extinction ratio of 9.8 dB, which is sufficient for practical applications. The asymmetry of the eye diagram is due to the nonlinearity of the transfer function of the EAM, depending on the bias.

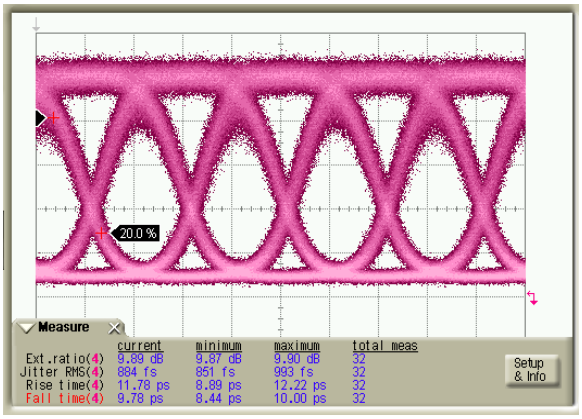

Fig. 5. 50 Gb/s NRZ eye diagram at λ = 1550 nm with 2^{31}-1 PRBS pattern for a 100 μm long hybrid silicon TW-EAM. The modulator was biased at −3 V with a driving voltage swing of only 2 V.

4. Conclusions

In summary, a hybrid silicon TW-EAM with a modulation bandwidth of 42 GHz and a steady-state extinction ratio larger than 11 dB has been reported. The open eye diagram obtained at 50 Gb/s presents a dynamic extinction ratio of 9.8 dB, with a driving votage swing of only 2 V. To the best of our knowledge, this is the fastest silicon-based modulator demonstrated and can be integrated with hybrid silicon lasers for high-speed optical interconnects.

Acknowledgments

This work is under financial support from Intel and the DARPA/MTO PICO Center. The authors thank Scott Rodgers, Mario Paniccia and Ling Liao for useful discussions.

#141070 - $15.00 USD Received 13 Jan 2011; revised 25 Feb 2011; accepted 4 Mar 2011; published 14 Mar 2011